Converter Topology with Load-Neutral Modulation for Trapezoidal-EMF PM Motor Drives

Federico Caricchi, *Member, IEEE,* Fabio Crescimbini, *Member, IEEE,* and Thomas A. Lipo, *Fellow, IEEE*

***Abstract*— The average torque of concentrated winding PM machines can be increased significantly by supplying current waveforms matching in full the trapezoidal back EMF. However, such current supply arrangements involve a large harmonic current flowing into the machine neutral. This paper presents an innovative converter topology to overcome the problem. This new configuration extends the standard layout of conventional PWM-VSI by adding a fourth branch devoted to control the voltage of the machine neutral. The inverter modes of operation resulting from the modulation of the machine neutral are discussed, and the paper reports the experimental results achieved from a converter prototype which has been constructed using IGBTs. Results show that the new inverter configuration allows significant benefits in the machine average torque, as well as the fact that the machine neutral modulation introduces an additional degree of freedom in the machine torque control.**

I. Introduction

APPLICATIONS of concentrated winding machines in electrical drives have prompted a number of significant problems which concern the design of both the machine and the power converter supplying the machine. As an example, for low-speed high-torque applications, an axial-flux PM motor has been proposed [1]. This machine is characterized by a high number of poles. The design of the machine with a torque/weight ratio as high as possible is mandatory in order to increase the machine power density and efficiency, as well as to reduce the costs. Further advantages can be achieved from a suitable arrangement of the machine supply. In fact, the performance of such concentrated winding PM drives can be improved greatly in terms of average output torque if the machine is fed by means of current waveforms which allow full contribution of the machine back EMF waveform in producing torque, such as in the case of a supply arrangement using either full square-wave or trapezoidal current waveforms. Such an approach, however, requires a suitable power converter configuration, since a large harmonic current flows in the machine neutral resulting from star connection of the stator winding.

This paper deals with an innovative converter topology which permits shaping of the machine current supply, so that the converter output current waveform can be adjusted suitably with respect to the machine back EMF. This new configuration extends the standard layout of PWM-Voltage Stiff Inverters by adding a fourth branch, which is devoted to control the voltage of the machine neutral. The paper describes the inverter modes of operation and reports experimental results from a converter prototype which has been constructed using IGBTs rated 600 V, 25 A.

Manuscript received August 25, 1992; revised November 5, 1993.

F. Caricchi and F. Crescimbini are with the Department of Electrical Engineering, University of Rome "La Sapienza," Via Eudossiana, 18-00184, Rome, Italy.

T. A. Lipo is with the Department of Electrical and Computer Engineering, University of Wisconsin–Madison, Madison, WI 53706 USA.

IEEE Log Number 9400096.

II. Torque Mechanism in PM Machines

Benefits resulting from different current supply arrangements of a concentrated winding PM motor can be evaluated simply by assuming square-wave air-gap flux density, idealized current control, and machine operation with a large inertia load. Although in the following the analysis is specialized to axial-flux PM motors, the issues lead to general conclusions, which thereby can be extended to conventional radial-flux concentrated winding PM motors. In developing the analysis, fixed machine design characteristics are taken into account, such as the PM's geometry and the machine total number of turns. Hence, the machine average torque (T_{ave}) is evaluated considering different current supply arrangements, which result from both the number of the machine phases (m) and the shape of the commanded phase current waveform.

A. Machine Back EMF

With the assumptions indicated above, the EMF waveform can be derived easily from either the flux cutting or the flux linking method. Considering an axial-flux motor having PM's over all the pole pitch of its stator winding, the peak value of the phase back EMF can be written as

$$E_{pk} = \frac{E_{\max}}{m} \tag{1}$$

where

$$E_{\max} = N\omega_r B_{\text{ave}}(R_o^2 - R_i^2) \tag{2}$$

represents the maximum open-circuit peak voltage achievable from connecting in series all the machine turns, and

- N total number of turns for all m phases
- ω_r mechanical rotor speed
- B_{ave} average air-gap flux density
- R_o outside radius of the magnet
- R_i inside radius of the magnet.

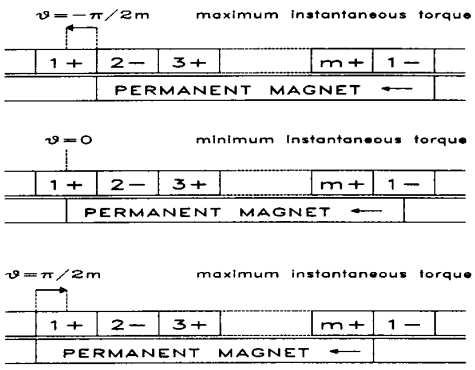

Fig. 1. Schematic representation of the commutation process in a concentrated winding PM motor: the coils of the machine phase 1 are under commutation through the interpolar axis.

Because each machine phase is realized by connecting in series concentrated coils equal to the number of the machine poles, the analysis can be restricted to only one pole of the machine and one coil per pole and per phase, as shown in Fig. 1. Such a machine configuration produces a phase back EMF having a trapezoidal waveform, which remains constant at E_{pk} along a portion $(m-1)/m$ of the pole pitch, whereas it changes linearly when the coil of the phase under consideration is commutating through the interpolar axis.

It can be recognized from Fig. 1 that at any given time instant there is always one coil under commutation, and this commutation process can be described by introducing an abscissa ϑ, which represents the position of the coil under commutation with respect to the interpolar axis. Hence, during the commutation interval, the phase EMF waveform can represented by the expression

$$e_{ph}(\vartheta) = \frac{2E_{\max}}{\pi}\,\vartheta \tag{3}$$

while the coil position ϑ changes linearly (i.e., ω_r is a constant) from $-\vartheta^*$ to $+\vartheta^*$, being $\vartheta^* = \pi/2m$.

The results given by (1) and (3) will prove useful later on. They clearly indicate that for fixed machine design characteristics both the EMF peak value and the commutation interval π/m decrease as the machine number of phases increases, whereas the slope of the EMF trapezoidal waveform does not depend on the value of m. However, the portion of the pole pitch in which the EMF is at its peak value increases in accordance with the machine number of phases.

B. Machine Torque

Assuming idealized current control allows a considerable insight into the machine torque production process. Whatever current control of a concentrated winding PM motor is performed, it can be recognized that the desired peak current (I_{pk}) should be supplied to a given machine phase during the time interval in which the phase coils are completely under the action of the poles, and thereby the phase EMF waveform is at its peak value E_{pk}. By such an approach, it clearly appears that the maximum instantaneous torque is achieved at the time instant when the coils of all the machine phases are completely under the poles (i.e., at either $\vartheta = -\pi/2m$ or $\vartheta = \pi/2m$) so that all phases may give the maximum contribution in producing torque. On the contrary, the minimum instantaneous torque occurs whenever the coils of one of the m machine phases cross the interpolar axis (i.e., at $\vartheta = 0$), and thereby the relative instantaneous phase EMF becomes zero.

Hence, the above considerations suggest that the machine instantaneous torque can be described by means of a periodic time function whose period corresponds to changes of ϑ from $-\pi/2m$ to $\pi/2m$. Thereby, the period of the torque waveform depends on the machine number of phases, whereas the shape of such a waveform is fixed by the current control strategy. Considering that at any given time instant there is always one of the machine phases commutating gives an expression for the air-gap instantaneous power related to the machine torque as

$$P_{ag}(\vartheta) = (m-1)E_{pk}I_{pk} + e_{ph}(\vartheta)i_{ph}(\vartheta) \tag{4}$$

where $e_{ph}(\vartheta)$ is given by (3), and

$$i_{ph}(\vartheta) = K(\vartheta)I_{pk} \tag{5}$$

represents the current that may be commanded to flow in the machine phase under commutation. The function $K(\vartheta)$ is introduced in order to take into account the shape of the current waveform.

Substituting (1), (3), and (5) into (4), the air-gap instantaneous power can be expressed in per-unit of the power $E_{\max}I_{pk}$, which represents the instantaneous air-gap power of a PM machine having an infinite number of phases (i.e., an equivalent PM dc motor). Hence, the per-unit instantaneous torque can be written as

$$T(\vartheta) = \frac{m-1}{m} + \frac{2}{\pi}\,\vartheta\,K(\vartheta) \tag{6}$$

whereas averaging this expression from $-\pi/2m$ to $\pi/2m$ gives the machine average torque

$$T_{\text{ave}} = \frac{m-1}{m} + \frac{2m}{\pi^2}\int_{-\pi/2m}^{\pi/2m} \vartheta K(\vartheta)\,d\vartheta. \tag{7}$$

The maximum and minimum p.u. values of the instantaneous torque can be calculated from (6) by setting $\vartheta = \pi/2m$ and $\vartheta = 0$, respectively; it yields

$$T_{\max} = 1 - \frac{1}{m}\left[1 - K\left(\frac{\pi}{2m}\right)\right] \tag{8}$$

$$T_{\min} = 1 - \frac{1}{m}. \tag{9}$$

Equations (8) and (9) show that the maximum and minimum instantaneous p.u. values of the machine torque depend on the machine number of phases; in addition to that, (8) shows that the maximum instantaneous torque is determined also by the current that may be commanded to flow in the machine phases during the commutation through the interpolar axis. Hence, the machine current supply may be arranged suitably in order to increase the maximum instantaneous torque, although such a technique produces inherently a certain amount of torque

ripple, as the comparison between (8) and (9) indicates. Using (6) and (7) gives an expression of the torque ripple as

$$T_{pp}(\vartheta) = \frac{2}{\pi}\left[\vartheta K(\vartheta) - \frac{m}{\pi}\int_{-\pi/2m}^{\pi/2m} \vartheta K(\vartheta)\, d\vartheta\right]. \quad (10)$$

III. Improvements in the Machine Torque

Equation (7) puts into evidence the possible methods of increasing the machine average torque by means of a suitable choice for both machine number of phases and shape of the current waveform commanded in the machine phases. Conventional solutions used for supplying trapezoidal-EMF PM motors consider $K(\vartheta) = 0$, which means that each machine phase is fed by a current of a constant value I_{pk} only when the EMF is at its peak value E_{pk}. In this case, the phase current waveform results in a square wave having a width of 180 $(m-1)/m$ electrical degrees.

One advantage of machine supply arrangements using 180 $(m-1)/m$ square wave current waveforms is that the machine develops a constant instantaneous torque, as either (6) or (10) indicate clearly for $K(\vartheta) = 0$. In this case, however, the comparison between (9) and (8) reveals that this is merely the result of extracting from the machine only the minimum value of the torque that the machine can develop on an instantaneous basis. Hence, in this case, benefits over the machine performance rely on an increase of the minimum instantaneous torque given by (9), and thereby they can be accomplished only by choosing a machine number of phases as high as possible. As an example, a five-phase machine supplied by means of a 144 degree square-wave current waveform was proposed in [2], and it can be recognized easily from (7) that such a motor drive arrangement gives a 20% extra torque if compared to conventional three-phase motor drives.

For PM motor drives applications where the torque ripple is not a major concern (e.g., PM drives devoted to the propulsion of electrical vehicles), shaping of the phase current waveform with respect to the machine EMF allows an improvement of the machine average torque, as well as gives an additional degree of freedom in the drive torque control. Considering the second term of (7), it can be recognized that an extra average torque may be produced if at any given time instant current is allowed to flow in the machine phase under commutation, so that the relative EMF can contribute in producing torque before reaching its peak value. However, such an approach requires an innovative configuration of the power converter supplying the machine, since it can be demonstrated that, in this case, a harmonic current has to be allowed to flow in the machine neutral.

In the following, this paper discusses an innovative power converter topology to overcome the problem, so that the machine current control may be arranged considering a phase current having either a full square-wave waveform or a waveform matching the trapezoidal EMF of the machine. The first case corresponds to a current supply arrangement having $K(\vartheta) = 1$, whereas $K(\vartheta) = 2m\vartheta/\pi$ represents a machine supply resulting in a phase current trapezoidal waveform. Hence, the average torque given by (7) becomes

$$[T_{\text{ave}}]_{fsw} = 1 - \frac{1}{2m} \quad (11)$$

for a full square-wave current supply, whereas it yields

$$[T_{\text{ave}}]_{tw} = 1 - \frac{2}{3m} \quad (12)$$

in the case of a current trapezoidal waveform.

Equations (11) and (12) permit evaluation of the average torque improvement with respect to the conventional current supply arrangement which assumes $K(\vartheta) = 0$. It can be determined that a full square-wave current yields an increased average torque of $1/[2(m-1)]$ p.u., whereas a trapezoidal current waveform allows a torque gain of $1/[3(m-1)]$ p.u. The analysis shows also that benefits over the machine average torque decrease as the number of the machine phases increases. Thereby, in the following, only current supply arrangements devoted to three-phase PM machines are discussed, since they seem to result in the most significant torque relative gain.

Upon examining the issues of the analysis developed above, it should be noted that comparable torque benefits can be achieved by either increasing the machine number of phases or by allowing a current harmonic component in the machine neutral. To this purpose, the average torque values resulting from different current supply arrangements of a trapezoidal-EMF PM machine are indicated in Table I. This table considers commanded phase current waveforms having the same peak value but a different shape; for a given phase current waveform, the relative rms value can be calculated in per-unit of the current peak value as

$$I_{\text{rms}} = \sqrt{1 - \frac{1}{m} + \frac{1}{\pi}\int_{-\pi/2m}^{\pi/2m} K^2(\vartheta)\, d\vartheta} \quad (13)$$

and the current rms values related to different current supply arrangements are also reported in Table I for comparison purposes.

For three-phase current supply arrangements, Table I shows that a 25% extra torque is achieved from a 180 degree square wave current; whereas in the case of a 120 degree trapezoidal current waveform, the torque gain is about 16%, if compared to the conventional supply arrangement using a 120 degree square wave. Although a trapezoidal wave current having the same peak value as a 180 square wave current seems to result in a lower torque benefit, it can be noted from Table I that the trapezoidal waveform produces a larger average torque per rms amp. Hence, for applications where increased efficiency is important, the trapezoidal wave should be considered, since the resistive losses will be less for the same output power [3].

On the other hand, since the torque capability of a machine is limited by the machine heating, a further comparison among different current supply arrangement of a PM machine may consider current waveforms having a different shape but the same rms value. The last column of Table I proves to be useful for such a comparison, which can be carried out by assuming the rms value of 120 degree square-wave waveforms as reference. In this case, the comparative results indicate that three-phase 120 degree trapezoidal current waveforms give an

TABLE I
AVERAGE TORQUE (p.u.) OF A TRAPEZOIDAL-EMF PM MACHINE RESULTING FROM DIFFERENT CURRENT SUPPLY ARRANGEMENTS

Current Supply Arrangement	T_{ave}	Torque gain (%)	I_{rms}	T_{ave}/I_{rms}
$3\phi - 120$ degree sq. wave[a]	0.6667	(Ref.)	0.8165	0.8165
$3\phi - 120$ degree trap. wave[b]	0.7778	16.6	0.882	0.882
$3\phi - 180$ degree sq. wave[b]	0.8334	25.	1.	0.8334
$5\phi - 144$ degree sq. wave[a]	0.8	20. (Ref.)	0.8944	0.8944
$5\phi - 144$ degree trap. wave[b]	0.8667	30. (8.3)	0.931	0.931
$5\phi - 180$ degree sq. wave[b]	0.9	35. (12.5)	1.	0.9
Conventional CRPWM inverter topology.				
CRPWM inverter topology with load-neutral modulation.				

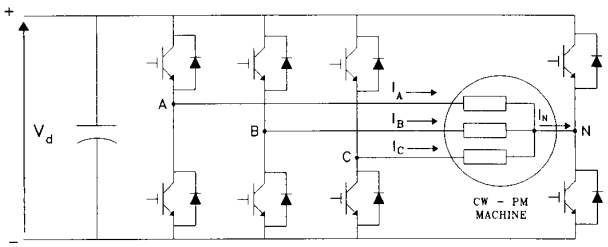

Fig. 2. Current regulated inverter with load-neutral modulation.

average torque which is 8% higher than the torque produced by the 120 degree square-wave current machine; whereas three-phase 180 degree square-wave waveforms result in a lower torque benefit, being only 2% the extra torque.

Effects of using the machine-neutral modulation technique for five-phase machines are also shown in Table I in comparison to both the conventional current supply arrangement of three-phase motor drives and the five-phase 144 degree square-wave phase current waveforms discussed in [2]. It is shown that both full square-wave and trapezoidal waveforms allow a further improvement in the average torque of five-phase machines, with 8.3% being the extra torque due to a trapezoidal current waveform and 12.5% the torque gain resulting from a full square-wave current waveform. Hence, increasing the machine phases from three to five should be taken into consideration if a machine average torque as high as possible is a mandatory requirement of the drive; although such a solution leads to a power converter of higher cost which may not be justified completely by the resulting extra torque of the machine.

IV. CONVERTER CONFIGURATION

As mentioned above, a large current harmonic component has to be allowed to flow in the machine neutral if a PM motor

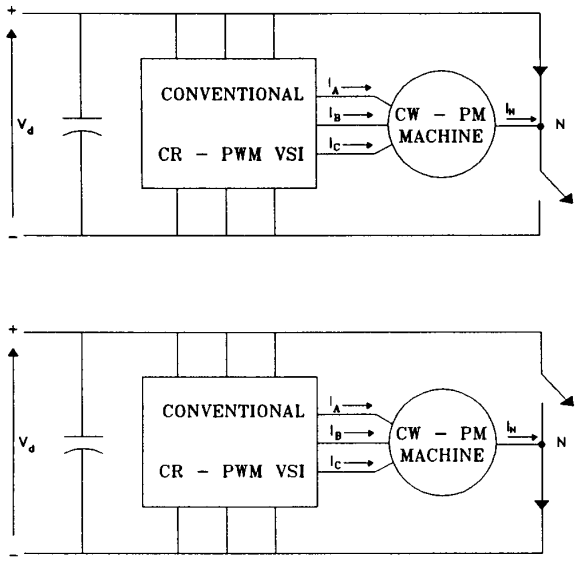

Fig. 3. Inverter extra modes due to the load-neutral modulation.

is supplied by means of either full square-wave or trapezoidal phase current waveforms. Hence, the machine neutral has to be connected to the inverter dc link and, furthermore, the control of the current waveform in the machine phases requires that the average value of the neutral voltage must (on the average) be kept at half the value of the dc link voltage.

For three-phase PM machines, these problems can be resolved by the converter topology shown in Fig. 2. This new configuration results from the standard layout of a three-phase VSI by adding a fourth branch devoted to control suitably the voltage of the machine neutral. The inverter branches connected to the machine input terminals can be operated in either six-step or PWM mode, whereas the fourth branch acts to modulate the neutral voltage so that the required average value is achieved. In order to reduce the current ripple resulting from the modulation, the switching frequency of the neutral-connected branch should be chosen several times higher than the inverter output frequency. Considering the converter modes of operation, it appears that adding the fourth branch splits up each mode related to operation of conventional square-wave VSI or PWM-VSI into two extra modes, which are due to connecting the neutral alternately to the positive and negative bus of the dc link, as shown schematically in Fig. 3.

V. EXPERIMENTAL STUDY

In order to demonstrate the feasibility of the approach, a PWM inverter having the topology shown in Fig. 2 was assembled using IGBT modules rated 600 V, 25 A. This converter prototype was used to drive a 16-pole axial-flux PM motor rated 32 N m [1], which has two Nd-Fe-B rotor discs and a slotless toroidal core supporting a three-phase concentrated winding.

A. Machine EMF Harmonic Content

Fig. 4(a) shows the open-circuit voltage waveforms of the machine prototype used for the experimental study. These

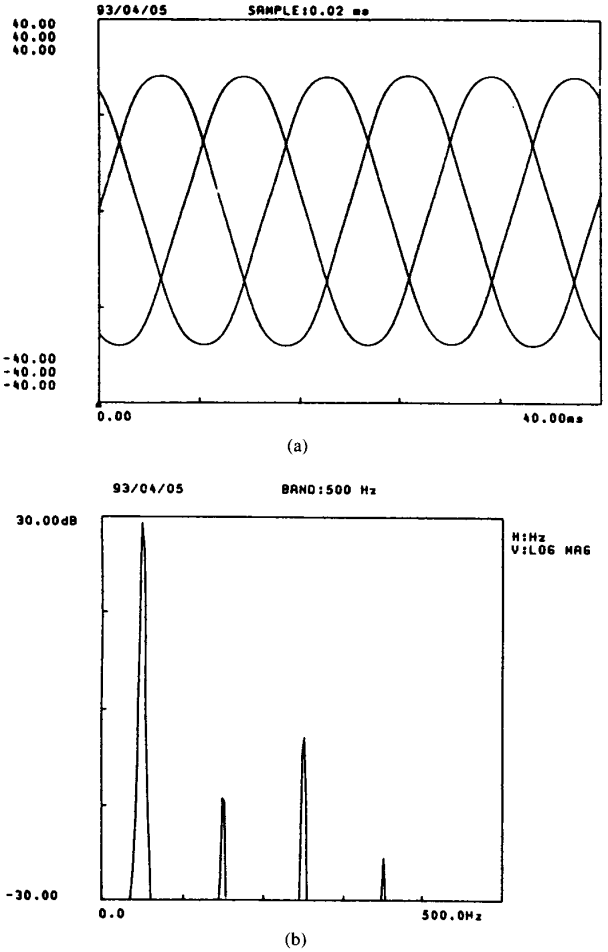

Fig. 4. Open circuit voltage of the axial-flux PM motor prototype: (a) EMF three-phase waveforms at 375 rpm (voltage scale 20 V/div, time scale 8 ms/div); (b) harmonic spectrum of the machine EMF waveforms.

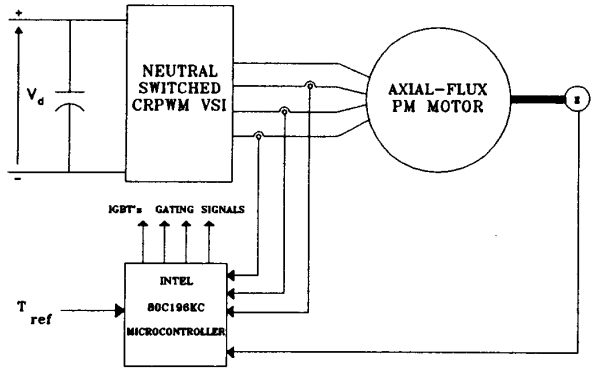

Fig. 5. Experimental arrangement of an axial-flux PM motor drive with load-neutral modulation.

EMF waveforms have a peak value of approximately 28 V at the rated speed of 375 rpm and the harmonic spectrum shown in Fig. 4(b). In comparison to the EMF trapezoidal waveform considered in the theoretical analysis developed previously, the

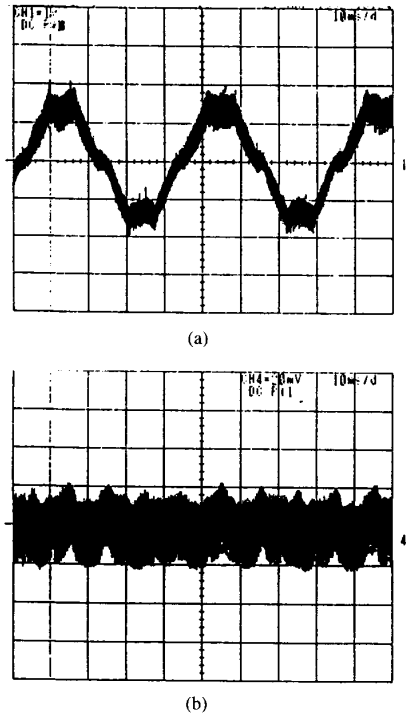

Fig. 6. Phase (a) and neutral (b) currents due to a commanded 60 degree trapezoidal current waveform (current scale: 10 A/div; time scale: 10 ms/div).

machine prototype EMF waveforms have a reduced harmonic content, and this fact limits the torque gain when applying the machine neutral voltage modulation technique discussed above. The reduced harmonic content of the machine prototype EMF waveforms is unfortunately the result of the particular arrangement of the machine PM poles, which occupy only 2/3 of the stator winding pole pitch measured at the medium radius of the toroidal core.

From a theoretical point of view, this fact can be put into evidence by evaluating the harmonic content of general EMF waveforms resulting from PM poles having a width $w_m = k_m\pi$, where k_m has a value chosen between $(1-1/m)$ and 1 in order to ensure that at any given time instant at least $(m-2)$ machine phases are completely under the machine poles. From such an assumption, it can be recognized that the machine EMF waveform remains constant at the peak value along a portion $(k_m - 1/m)$ of the pole pitch, whereas it changes linearly when the given machine phase commutates through the interpolar axis. That is, the position ϑ with respect to the interpolar axis changes from $-\vartheta^*$ to $+\vartheta^*$, being in this case $\vartheta^* = \pi/2m + \pi(1-k_m)/2$. Applying Fourier analysis yields the magnitude of the n-order EMF harmonic component as

$$e_n = \frac{4}{\pi} E_{pk} \frac{\sin(n\vartheta^*)}{n^2\vartheta^*} \qquad (\text{for } n \text{ odd}) \tag{14}$$

and thereby the p.u. magnitude with respect to the fundamental component e_1 is

$$\frac{e_n}{e_1} = \frac{1}{n^2} \frac{\sin(n\vartheta^*)}{\sin\vartheta^*} \qquad (\text{for } n \text{ odd}). \tag{15}$$

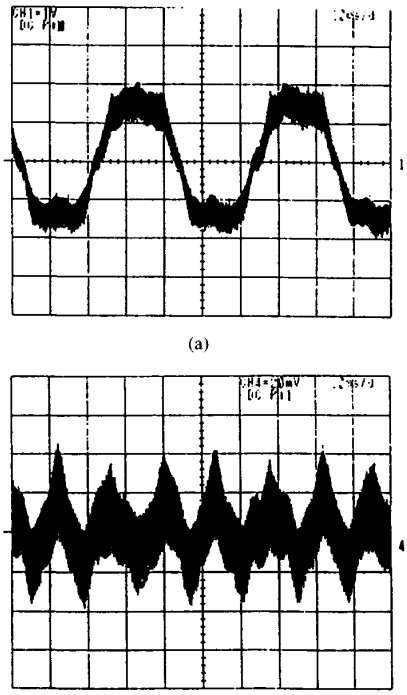

(a)

(b)

Fig. 7. Phase (a) and neutral (b) currents due to a commanded 120 degree trapezoidal current waveform (current scale: 10 A/div; time scale: 10 ms/div).

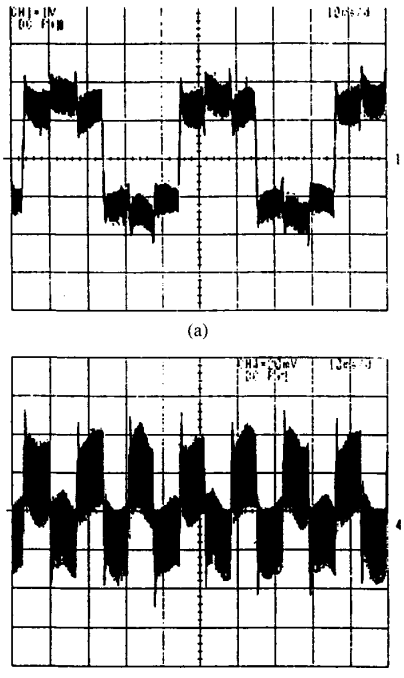

(a)

(b)

Fig. 8. Phase (a) and neutral (b) currents due to a commanded 180 degree square-wave current waveform (current scale: 10 A/div; time scale 10 ms/div).

Whenever specialized for three-phase EMF trapezoidal waveforms related to PMs distributed along the full stator winding pole pitch, as shown previously in Fig. 1, equation (15) gives an EMF waveform harmonic content comprising a 22% third harmonic, whereas the fifth and seventh harmonic components are 4 and 2%, respectively. On the other hand, if the PMs occupy only 2/3 of the stator winding pole pitch, the third harmonic component disappears from the resulting three-phase EMF waveforms, while both the fifth and seventh harmonics have again the magnitudes indicated above.

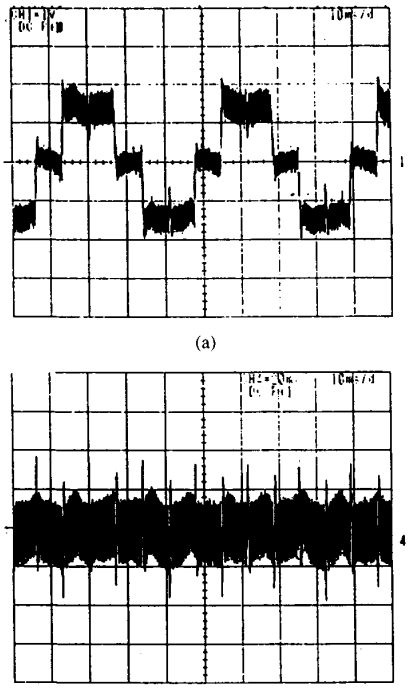

(a)

(b)

Fig. 9. Phase (a) and neutral (b) currents due to a commanded 120 degree square-wave current waveform (current scale: 10 A/div; time scale: 10 ms/div).

Hence, it appears clearly that benefits over the machine torque resulting from the modulation of the machine neutral voltage depend mainly on the magnitude of the EMF third harmonic component, and thereby this fact should be taken into consideration properly when designing a PM machine to be fed by the converter shown in Fig. 2. The machine prototype used for the experimental study was not designed with such a particular current supply arrangement in mind, and thereby the machine prototype EMF waveforms have a poor relatively third-harmonic content, which is merely the result of a nonsquare-wave flux-density distribution at the machine airgap.

B. Experimental Results

Fig. 5 shows schematically the drive configuration used during the experimental tests. For purposes of motor control, an INTEL 80C196KC microcontroller is employed together with a 5000 ppr encoder and Hall-effect transducers for sensing the rotor speed and the phase currents, respectively. The control algorithm implements the conventional PWM strategy,

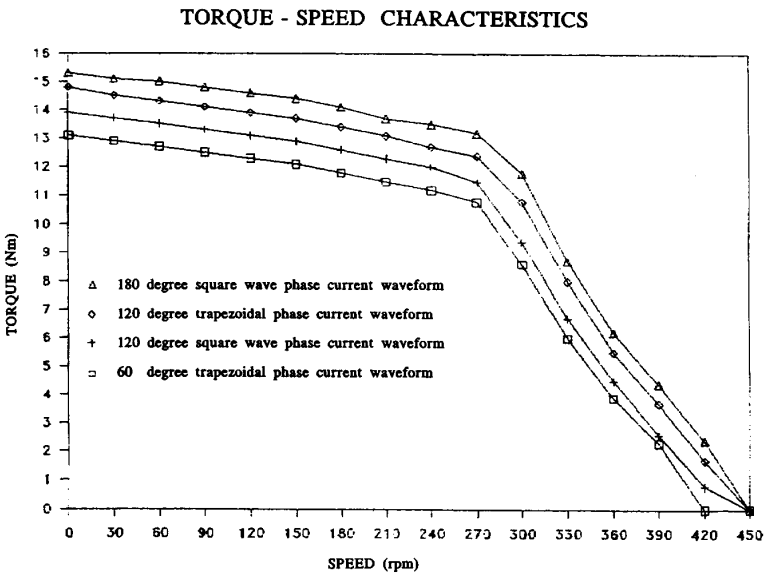

Fig. 10. Average torque versus rotor speed characteristics of the axial-flux PM motor drive prototype with load-neutral modulation.

by using a 15-kHz saw-tooth carrier and control signals resulting from the error between the controller commanded phase currents and the actual motor currents. The neutral-connected inverter branch is switched at the same frequency of the saw-tooth carrier, by using a fixed duty-cycle value of 0.5 as required.

Because the EMF waveforms of the machine prototype remain constant along intervals of approximately 60 electrical degree, it was decided to carry out the experimental study by considering commanded three-phase current waveforms as follows:

1) 60 degree trapezoidal current waveform matching the machine EMF waveform;
2) 120 degree trapezoidal current waveform which changes by a slope twice that one of the EMF waveform;
3) 180 degree square-wave current waveform;
4) 120 degree square-wave current waveform, which approximates the current supply of conventional three-phase CRPWM-VSI—in this case, the modulation strategy was operated in order to achieve a zero average current during the 60 degree commutation angle.

With reference to above-indicated current supply arrangements a), b), c), and d), oscilloscope traces resulting from the experimental study are shown in Figs. 6–9. These results were achieved running the machine at 180 rpm under a shaft load due to a controllable dc brake, and all figures refer to a commanded peak current of 14 A.

Experimental current waveforms show a significant phase current ripple which reflects on a ripple of the neutral current greater than expected. This appeas to be the result of the low value of the machine leakage inductance (i.e., about 220 μH), but it can also be a result of the microcontroller execution time, which would not be reduced below about 100 μs/cycle. Inspection of experimental waveforms also reveals the influence of the mutual inductance between machine phases on the phase current waveform. This is due to the current flowing in the machine neutral, and the phenomenon is particularly prominent in the case of supply currents having square wave waveform because of the resulting high value of the di/dt during current commutations.

Experimental data were additionally obtained for several load conditions of the PM drive prototype. Results are summarized in Fig. 10, which illustrates the steady-state average torque versus rotor speed characteristics related to each of the current supply arrangements indicated above. Benefits over the machine average torque due to the modulation of the machine neutral clearly appear, although the results shown in Fig. 10 indicate torque improvements less than expected. This fact is a consequence of the machine prototype characteristics, such as the poor harmonic content of the flux-density distribution at the machine airgap, as discussed previously.

VI. Conclusions

In comparison to the conventional solution used for trapezoidal-EMF PM motor drives, this paper has discussed different current supply arrangements in terms of machine number of phases and commanded phase current waveform. It has been shown that benefits over the machine average torque can be achieved if the motor is fed by means of phase current waveforms which allow full contribution of the machine back EMF waveform in producing torque, such as in the case of machine supply arrangements resulting in a large current harmonic component in the machine neutral. Such an approach requires a suitable power converter configuration, and this paper has presented an innovative converter topology which permits suitable adjustment of the converter output current with respect to the machine back EMF. This new configuration extends the standard topology of PWM-Voltage

Stiff Inverters by adding a fourth branch which is devoted to control of the voltage of the machine neutral.

In order to investigate the inverter modes of operation, an experimental study has been carried out driving an axial-flux PM motor by means of a converter prototype, which has been constructed using IGBTs rated at 600 V, 25 A. Conclusions prove the feasibility of shaping suitably the phase current waveform of PM motors by modulating the machine neutral, and such a possibility introduces an additional degree of freedom in the machine torque control. While benefits over the machine average torque have been experimented from the converter topology discussed in this paper, the experience gained from the construction of the PM drive prototype indicates that the drive overall cost is frequently determined mainly from the cost of the rare-earth PMs, so that the converter extra cost due to adding a fourth inverter branch could be a relatively negligible cost increment.

REFERENCES

[1] F. Caricchi, F. Crescimbini, A. Di Napoli, O. Honorati, T. A. Lipo, G. Noia, and E. Santini, "Development of an IGBT inverter driven axial-flux PM synchronous motor drive," in *Proc. 4th EPE Conf.*, vol. 3, Florence, Italy, Sept. 3–6, 1991, pp. 482–487.

[2] H. Toyliyat, L. Y. Xu, and T. A. Lipo, "A five phase reluctance motor with high specific torque," in *Proc. 1990 IEEE Ind. Appl. Conf. Annu. Meet.*, vol. 1, Seattle, WA, Oct. 7–12, 1990, pp. 207–213.

[3] C. C. Jensen, F. Profumo, and T. A. Lipo, "A low loss permanent magnet brushless dc motor utilizing tape wound amorphous iron," in *Proc. 1990 IEEE Ind. Appl. Conf. Annu. Meet.*, vol. 1, Seattle, WA, Oct. 7–12, 1990, pp. 281–286.

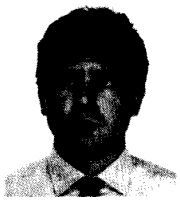

Federico Caricchi (M'91) received the electrical engineering degree from the University of Rome "La Sapienza," Rome, in 1988.

From 1988 to 1990 he was an Officer in the Italian Navy and he was involved in the analysis of high-speed gen-sets. Since 1991 he has been with the Department of Electrical Engineering, University of Rome "La Sapienza," where he is currently an Assistant Professor. His research interests are in analysis and design of unconventional electric machines and PM motor drives.

Dr. Caricchi is a member of the Italian Association of Electric and Electronics Engineers (AEI), and the Italian Association for Naval Techniques (ATENA).

Fabio Crescimbini (M'91) received the electrical engineering degree and Ph.D. degree in electrical engineering from the University of Rome "La Sapienza," Rome, in 1982 and 1987, respectively.

He was a Visiting Scholar at the Department of Electrical and Computer Engineering, University of Wisconsin, Madison, in 1986. His experience includes working in the field of telecommunication apparatus systems as an Officer in the Italian Army, and working in design and installation of UPS systems as an Electrical Engineer in a private company. Since 1989 he has been with the Department of Electrical Engineering of the University of Rome "La Sapienza," where he is involved in the research of power electronics and machine drives. His current research activities are in analysis and design of power converter topologies for unconventional applications such as EVs, motor drives, and renewable energy generating systems.

Dr. Crescimbini is a member of the European Power Electronics Association.

Thomas A. Lipo (F'87) received the B.E.E. and M.S.E.E. degrees from Marquette University, Milwaukee, WI, in 1962 and 1964, respectively, and the Ph.D. degree in electrical engineering from the University of Wisconsin in 1968. He was an NRC Postdoctoral Fellow at the University of Manchester Institute of Science and Technology, Manchester, England, from 1968 to 1969.

From 1969 to 1979 he was an Electrical Engineer in the Power Electronics Laboratory of Corporate Research and Development of the General Electric Company, Schenectady, NY. He became Professor of Electrical Engineering at Purdue University, West Lafayette, IN, in 1979 and later joined the University of Wisconsin, Madison, in the same capacity. He has been involved in the research of power electronics and ac drives for over 25 years.

Dr. Lipo has received 11 IEEE prize paper awards including co-recipient of the Best Paper Award in IEEE TRANSACTIONS ON INDUSTRY A PPLICATIONS for 1984. In 1986 he received the Outstanding Achievement Award from the IEEE Industry Application Society for his contributions to the field of ac drives.